diabetes®
American Diabetes Association®

Stromal Interaction Molecule 1 Maintains β-Cell Identity and Function in Female Mice Through Preservation of G-Protein–Coupled Estrogen Receptor 1 Signaling

Paul Sohn, Madeline R. McLaughlin, Preethi Krishnan, Wenting Wu, Marjan Slak Rupnik, Akira Takasu, Toshiya Senda, Chih-Chun Lee, Tatsuyoshi Kono, and Carmella Evans-Molina

Diabetes 2023;72(10):1433–1445 | https://doi.org/10.2337/db22-0988

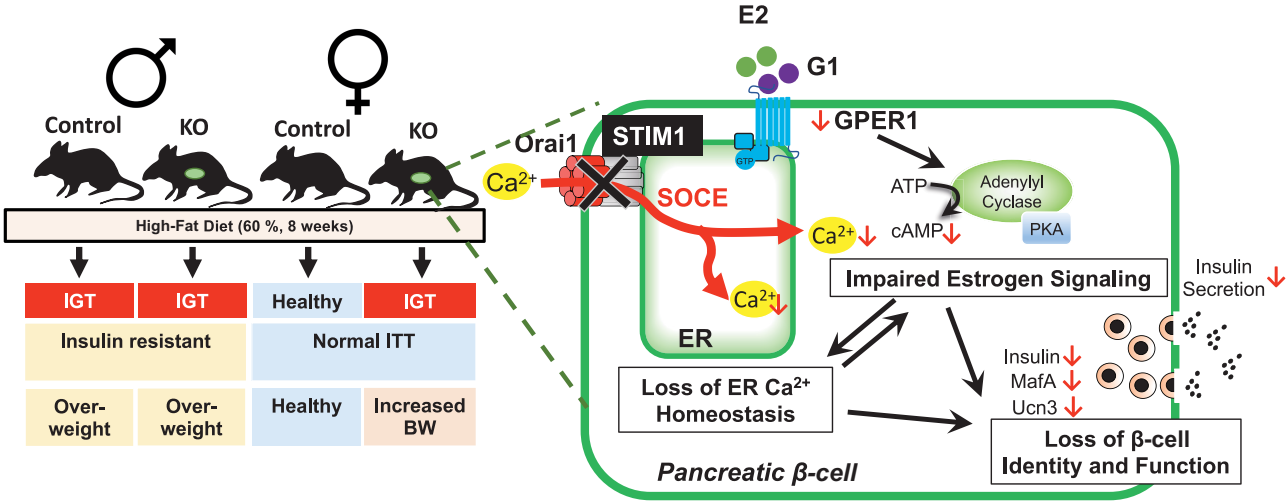

STIM1 maintains β-cell identity and function in female mice through preservation of endoplasmic reticulum calcium homeostasis and GPER1 signaling. A sexually dimorphic phenotype was observed when STIM1 was deleted in the β-cell and mice were challenged with high-fat diet for 8 weeks. Impaired glucose tolerance in female mice was accompanied by reductions in β-cell mass and identity and lower serum insulin levels. Mechanistic assays demonstrated that STIM1 maintains β-cell function and identity through GPER1-mediated estradiol signaling. BW, body weight; IGT, impaired glucose tolerance; ITT, insulin tolerance test; KO, knockout.

Stromal Interaction Molecule 1 Maintains β-Cell Identity and Function in Female Mice Through Preservation of G-Protein–Coupled Estrogen Receptor 1 Signaling

Paul Sohn,[1,2,3] Madeline R. McLaughlin,[4,5] Preethi Krishnan,[2,4,6] Wenting Wu,[2,7] Marjan Slak Rupnik,[8,9] Akira Takasu,[10] Toshiya Senda,[10] Chih-Chun Lee,[2,3,4] Tatsuyoshi Kono,[2,3,4,11] and Carmella Evans-Molina[1,2,3,4,11,12,13]

Diabetes 2023;72:1433–1445 | https://doi.org/10.2337/db22-0988

Altered endoplasmic reticulum (ER) Ca^{2+} signaling has been linked with β-cell dysfunction and diabetes development. Store-operated Ca^{2+} entry replenishes ER Ca^{2+} through reversible gating of plasma membrane Ca^{2+} channels by the ER Ca^{2+} sensor, stromal interaction molecule 1 (STIM1). For characterization of the in vivo impact of STIM1 loss, mice with β-cell–specific STIM1 deletion (STIM1Δβ mice) were generated and challenged with high-fat diet. Interestingly, β-cell dysfunction was observed in female, but not male, mice. Female STIM1Δβ mice displayed reductions in β-cell mass, a concomitant increase in α-cell mass, and reduced expression of markers of β-cell maturity, including MafA and UCN3. Consistent with these findings, STIM1 expression was inversely correlated with HbA_{1c} levels in islets from female, but not male, human organ donors. Mechanistic assays demonstrated that the sexually dimorphic phenotype observed in STIM1Δβ mice was due, in part, to loss of signaling through the noncanonical 17-β estradiol receptor (GPER1), as GPER1 knockdown and inhibition led to a similar loss of expression of β-cell maturity genes in INS-1 cells. Together, these data suggest that STIM1 orchestrates pancreatic β-cell function and identity through GPER1-mediated estradiol signaling.

ARTICLE HIGHLIGHTS

- Store-operated Ca^{2+} entry replenishes endoplasmic reticulum (ER) Ca^{2+} through reversible gating of plasma membrane Ca^{2+} channels by the ER Ca^{2+} sensor, stromal interaction molecule 1 (STIM1).
- β-Cell–specific deletion of STIM1 results in a sexually dimorphic phenotype, with β-cell dysfunction and loss of identity in female but not male mice.
- Expression of the noncanonical 17-β estradiol receptor (GPER1) is decreased in islets of female STIM1Δβ mice, and modulation of GPER1 levels leads to alterations in expression of β-cell maturity genes in INS-1 cells.

Type 2 diabetes (T2D) affects over 537 million individuals worldwide and develops as a result of peripheral insulin resistance and pancreatic β-cell dysfunction (1,2). The

[1]Department of Anatomy, Cell Biology, and Physiology, Indiana University School of Medicine, Indianapolis, IN
[2]Center for Diabetes and Metabolic Diseases, Indiana University School of Medicine, Indianapolis, IN
[3]Herman B Wells Center for Pediatric Research, Indiana University School of Medicine, Indianapolis, IN
[4]Department of Pediatrics, Indiana University School of Medicine, Indianapolis, IN
[5]Weldon School of Biomedical Engineering, Purdue University, West Lafayette, IN
[6]Department of Chemical and Biological Engineering, University of British Columbia, Vancouver, Canada
[7]Department of Medical and Molecular Genetics, Indiana University School of Medicine, Indianapolis, IN
[8]Center for Physiology and Pharmacology, Medical University of Vienna, Vienna, Austria
[9]Institute of Physiology, Faculty of Medicine, University of Maribor, Maribor, Slovenia
[10]Structural Biology Research Center, Institute of Materials Structure Science, High Energy Accelerator Research Organization, Ibaraki, Japan
[11]Richard L. Roudebush Veterans' Administration Medical Center, Indianapolis, IN
[12]Department of Biochemistry and Molecular Biology, Indiana University School of Medicine, Indianapolis, IN
[13]Department of Medicine, Indiana University School of Medicine, Indianapolis, IN

Corresponding author: Carmella Evans-Molina, cevansmo@iu.edu, or Tatsuyoshi Kono, konot@iu.edu

Received 29 November 2022 and accepted 7 July 2023

This article contains supplementary material online at https://doi.org/10.2337/figshare.23710011.

majority of genetic variants associated with T2D risk are thought to act at the level of the β-cell, suggesting that certain "at-risk" individuals are more susceptible to β-cell failure in settings of insulin resistance such as obesity and pregnancy (3,4). In addition to genetic predisposition, systemic and local factors, including elevated levels of glucose, proinflammatory cytokines, and free fatty acids, directly contribute to impaired insulin secretion, β-cell death, and dedifferentiation (5,6).

Impairments in β-cell calcium (Ca^{2+}) signaling have been linked to a number of molecular pathways that lead to β-cell dysfunction and diabetes development. The fidelity of Ca^{2+} signaling requires the maintenance of steep concentration gradients, organized at both the cellular and organelle level. In the pancreatic β-cell, the endoplasmic reticulum (ER) serves as the dominant intracellular Ca^{2+} store (7), and high levels of Ca^{2+} within the ER are maintained by the balance of ER Ca^{2+} uptake by the sarco-endoplasmic reticulum Ca^{2+} ATPase (SERCA) pump and ER Ca^{2+} release through the ryanodine receptors (RYR) and inositol 1,4,5-triphosphate receptors (IP3R) (8–10). In response to ER Ca^{2+} depletion, a process known as store-operated calcium entry (SOCE) replenishes ER Ca^{2+} levels through a family of channels referred to as store-operated or Ca^{2+} release–activated channels. During SOCE, decreased ER Ca^{2+} concentrations are detected by stromal interaction molecule 1 (STIM1), an ER Ca^{2+} sensor. STIM1 oligomerizes and translocates to the ER/plasmalemmal junctional regions (11), where it complexes with Orai Ca^{2+} channels to promote influx of Ca^{2+} from the extracellular space into the cytoplasm and ultimately into the ER lumen (12,13).

SOCE has been accepted as a main pathway of Ca^{2+} entry into nonexcitable cells. However, the role of SOCE in excitable and secretory cells, such as the pancreatic β-cell, has been controversial. Recent studies have implicated SOCE in glucose- and GPR40-mediated potentiation of insulin secretion (14). We previously demonstrated reduced STIM1 mRNA and protein expression in islets from donors with T2D and in human islets and INS-1 β-cells treated with proinflammatory cytokines and palmitate, and we showed that STIM1 overexpression improves insulin secretion (15). However, whether STIM1 loss impacts in vivo responses to metabolic stressors, including diet-induced obesity, remains unexplored.

RESEARCH DESIGN AND METHODS

Animals

Male mice, strains B6(Cg)-Ins1$^{tm1.1(cre)Thor}$/J (Ins1-Cre) and B6(Cg)-Stim1^{tm1Rao}/J (STIM1$^{fl/fl}$), were purchased from The Jackson Laboratory, and colonies were established in our facility. Pancreatic β-cell–specific STIM1 knockout (STIM1Δβ) mice were generated through crossing of Ins1-Cre and STIM1$^{flox/flox}$ mice. These strains were genotyped with use of The Jackson Laboratory PCR protocols 25780 and 18406.

Cell Lines

The STIM1 knockout cell line (STIM1KO) (15), wild-type (WT) INS-1 832/13 cells (Research Resource Identifier [RRID] CVCL_7226), and the α-TC cell line (alphaTC1 Clone 9, CRL-2350, RRID CVCL_0150) are described in Supplementary Material.

Metabolic Studies

Mouse body weight and body composition were determined with the EchoMRI-500 Body Composition Analyzer (RRID SCR_017104; EchoMRI) (16). Mice were fed ad libitum with a high-fat diet (HFD) (60% kcal from fat, cat. no. D12492; Research Diets) starting at age 8 weeks. After 8 weeks of HFD, glucose tolerance tests (GTT) were performed after a 6-h fast followed by administration of 1.5 g D-glucose/kg lean mass i.p. (17). Insulin tolerance tests were performed after 4 h of fasting followed by administration of 0.75 units insulin/kg lean mass i.p. (Novo Nordisk). Blood glucose levels were measured with a Contour glucometer (Bayer).

Glucose-stimulated insulin secretion was measured in vivo following a 6-h fast. Serum was collected after injection of glucose (2 g/kg lean body mass i.p.). Insulin levels in serum and tissues were measured with a Mouse Insulin ELISA kit (Mercodia).

Isolation of Mouse Islets

Mouse pancreatic islets were isolated at indicated time points through collagenase digestion as previously described (15). Islets were cultured in phenol red–free, low-glucose DMEM supplemented with 10% charcoal-stripped FBS, 100 units/mL penicillin, 100 μg/mL streptomycin, and 2 mmol/L L-glutamine.

Immunoblotting

INS-1 cells (1.5×10^5) or mouse islets (100–125) were processed for immunoblot analysis, as described in Supplementary Material. Antibodies used are listed in Supplementary Table 1.

Quantitative RT-PCR

INS-1 cells (832/13) and mouse islets were washed with PBS, and total RNA was extracted with the RNeasy Plus Mini Kit (INS-1 cells) and RNeasy Plus Micro Kit (mouse islets) (QIAGEN). Total RNA was reverse transcribed (18). cDNA was subjected to quantitative RT-PCR (RT-qPCR) with use of SensiFAST SYBR Lo-ROX (Bioline) and a QuantStudio 3 thermocycler (Applied Biosystems). Relative RNA levels were established against β-actin mRNA with the comparative ΔΔCt method as previously described (15). Primer sequences are provided in the Supplementary Table 1.

Immunofluorescence and Morphometric Analysis

After euthanasia, mouse pancreata were rapidly removed and fixed for downstream staining and imaging, as described in Supplementary Material.

Transmission Electron Microscopy Analysis and Quantitation

Transmission electron microscopy (TEM) imaging of islets and INS-1 cells was performed at the Advanced Electron Microscopy Facility at the University of Chicago (Chicago, IL). Images were analyzed as described the Supplemental Material.

Tandem Mass Tag MS/MS Proteomic Analysis of INS-1 Cells

Four biological replicates of WT and STIM1KO INS-1 cells (832/13) were prepared for tandem mass tag mass spectrometry (MS)/MS proteomic analysis, as described in Supplementary Material.

mRNA Sequencing, Library Generation, and Data Analysis

Following 8 weeks of HFD, islets were isolated from control and STIM1Δβ female mice, and bulk RNA sequencing analysis was performed, as described in Supplementary Material.

Quantification of Intracellular cAMP Levels

Intracellular cAMP levels in INS-1 cells were measured with cAMP Gs dynamic homogeneous time-resolved fluorescence kit (Cisbio) and read on SpectraMax iD5 Multi-Mode Microplate Reader (Molecular Devices) with excitation at 314 nm and emission at 620 and 668 nm.

siRNA Transfection

INS-1 (832/13) cells ($\sim 0.5 \times 10^6$) were plated in a 12-well plate and transfected with 50 nmol/L of control RNA (Ambion) or a mixture of three siRNAs targeting *Gper1* gene (nos. 139733, s139734, s139735; Ambion) diluted in Lipofectamine 3000 (Invitrogen) and Opti-MEM I medium at 37°C. Cells were cultured for 48 h in INS-1 cell culture medium, and RNA was isolated for downstream analysis using the RNeasy Plus Mini Kit (Qiagen).

Treatment With GPER1 Agonist E_2 and Antagonist G-15

INS-1 (832/13) cells were plated at 0.5×10^6 cells per 12-well plate. After 48 h, medium was replaced with fresh medium or medium containing 0.1 μmol/L of GPER1 agonist E2 (Steraloids) or 15 μmol/L of GPER1 antagonist G-15 (19). Cells were cultured for 24 h and collected for total RNA isolation and RT-qPCR analysis. The same protocol, using 75 islets/well in a 6-well plate, was used for experiments with mouse islets.

Calcium Imaging

Calcium imaging was performed in isolated islets as previously described (9). Data were analyzed as described in Supplementary Material.

Quantification and Statistical Analysis

Statistical analysis was performed with Prism 8.2.0 software (GraphPad Software) (RRID SCR_002798). For comparison of two data sets, two-tailed Student *t* test was used. For experiments involving three independent groups, data were analyzed with one-way ANOVA. Glucose and insulin tolerance tests were analyzed with two-way ANOVA followed by Tukey multiple comparison test. Results are reported as mean ± SEM. *P* value of <0.05 was considered to indicate a significant difference between groups.

Data and Resource Availability

Lead Contact

Requests for further information and requests for reagents should be directed to and will be fulfilled by the lead contact, C.E.-M.

Data and Code Availability

RNA-sequencing (RNA-seq) data generated during this study are available from the National Center for Biotechnology Information (NCBI) Gene Expression Omnibus (GEO) repository (no. GSE208135). Raw and searched MS data have been uploaded to MassIVE (MSV000089927).

RESULTS

β-Cell–Specific STIM1 Deficiency Does Not Alter Systemic Glucose Tolerance at 8 Weeks of Age

To define the impact of STIM1 loss in vivo, we generated a mouse model of β-cell–specific STIM1 knockout (STIM1Δβ) by crossing $STIM1^{fl/fl}$ mice (20) with mice constitutively expressing *Ins1*-cre (21). Appropriate genetic recombination was confirmed via PCR analysis (Supplementary Fig. 1*A* and *B*). Immunoblotting performed in islets isolated from control and STIM1Δβ mice demonstrated efficient deletion of STIM1 (Fig. 1*A*). Importantly, islets from STIM1Δβ mice did not show compensatory changes in mRNA expression of two main P-type ATPases responsible for β-cell ER Ca^{2+} uptake, *Serca2* and *Serca3*, or other SOCE molecular components, including *Stim2*, *Orai1*, and *Orai2* (Supplementary Fig. 1*C*).

At 8 weeks of age, lean and fat mass were identical between control and STIM1Δβ mice in both male and female cohorts (Fig. 1*B* and *C*). An intraperitoneal GTT showed no difference in systemic glucose homeostasis between control and STIM1Δβ mice in either males or females at this age (Fig. 1*D–F*).

β-Cell–Specific STIM1 Deficiency Increases Weight Gain and Fat Mass in HFD-Fed Female Mice

Beginning at age 8 weeks, male and female STIM1Δβ mice and littermate controls were fed HFD containing 60% of calories from fat. No differences in body weight gain were observed between male control and STIM1Δβ mice fed HFD for 8 weeks (Fig. 1*G*). However, after 6 and 8 weeks of HFD, female STIM1Δβ mice exhibited increased body weight compared with female control mice (Fig. 1*G*). After 8 weeks of HFD, there was no difference in lean mass between STIM1Δβ mice and controls in either males or females (Fig. 1*H*). Female HFD-fed STIM1Δβ mice had higher fat mass compared with HFD-fed female controls (Fig. 1*I*).

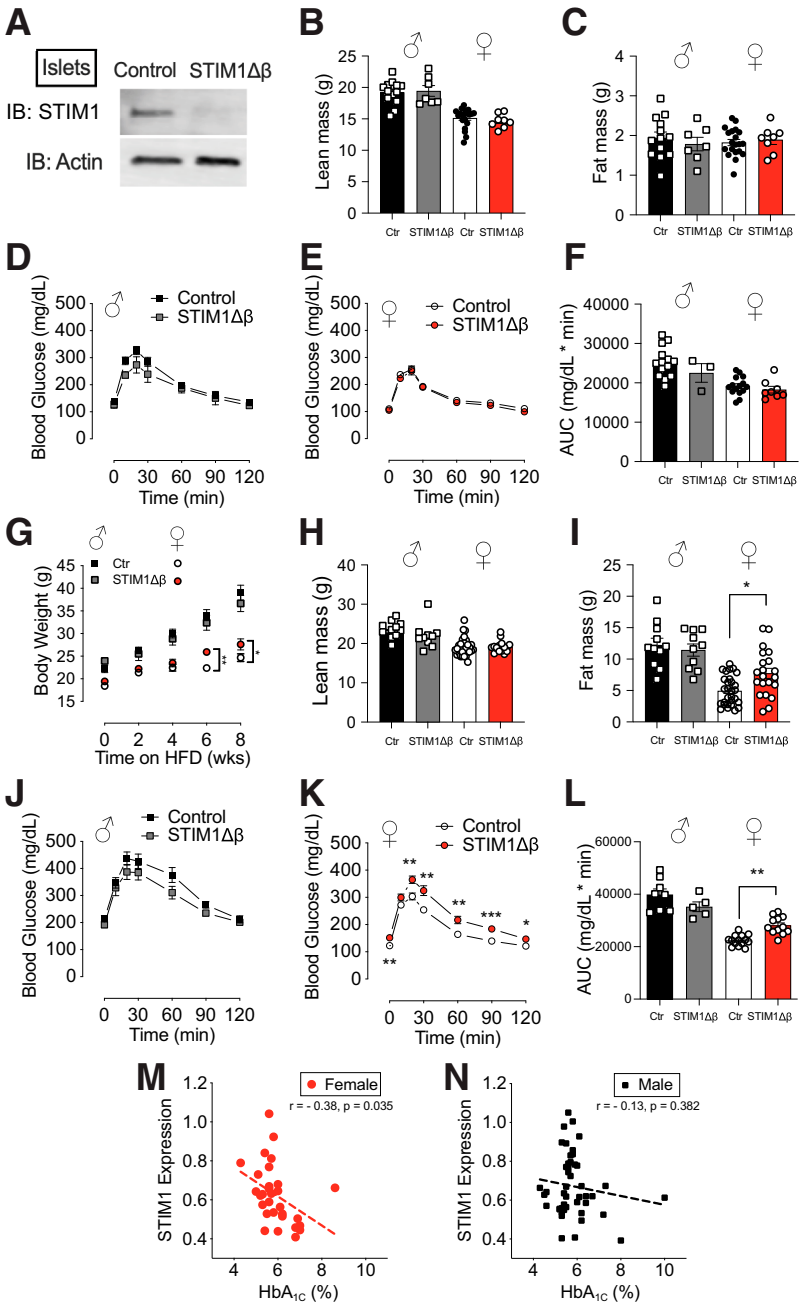

Figure 1—β-Cell–specific STIM1 deficiency causes glucose intolerance in female mice on HFD feeding. *A–F*: Control (STIM1$^{fl/fl}$ and unfloxed cre+) and STIM1Δβ mice were analyzed at 8 weeks of age. *A*: Immunoblot (IB) analysis of islets isolated from control and STIM1Δβ mice with use of anti-STIM1 and anti-actin antibodies. *B* and *C*: Lean (*B*) and fat (*C*) mass was measured with the EchoMRI-500 Body Composition Analyzer. *D–F*: GTT was performed (1.5 g/kg glucose dosed to lean mass) in male (*D*) and female (*E*) mice. *F*: GTT results were analyzed with area under curve (AUC) analysis. *G–L*: Control (Ctr) and STIM1Δβ mice were fed HFD containing 60% kcal from fat for 8 weeks, beginning at 8 weeks of age. *G*: Changes in body weight in male and female mice were monitored over the HFD feeding period. *H* and *I*: After HFD feeding for 8 weeks, lean (*H*) and fat (*I*) mass was measured with the EchoMRI-500 Body Composition Analyzer. *J–L*: GTT was performed (1.5 g/kg glucose dosed to lean mass) in male (*J*) and female (*K*) HFD-fed mice. *L*: Area under the curve analysis is shown graphically. Replicates are indicated with circles or squares; $n \geq 5$ in each group. Results are displayed as mean ± SEM. Indicated differences are statistically significant: $^*P < 0.05$, $^{**}P < 0.01$, $^{***}P < 0.001$. *M* and *N*: NCBI GEO data set (GSE50244) was retrieved for assessment of the relationship between STIM1 gene expression and clinical characteristics of female (*M*) and male (*N*) organ donors with and without T2D. The dotted line illustrates the correlation between STIM1 mRNA levels and HbA_{1c} levels in female organ donors. ($n = 35$; $r = -0.38$, $P = 0.035$.)

β-Cell–Specific STIM1 Deficiency Leads to Glucose Intolerance in Female HFD-Fed Mice

After 8 weeks of HFD, control and STIM1Δβ mice of both sexes were subjected to GTT, in which the dose of glucose was based on lean mass. Glucose tolerance was identical in male HFD-fed control and STIM1Δβ mice. In contrast, female HFD-fed STIM1Δβ mice had increased glucose excursions and worsened glucose tolerance in comparison

with control HFD-fed female mice (Fig. 1*J–L*). For determination of whether β-cell STIM1 ablation affected peripheral insulin sensitivity, an insulin tolerance test was performed in male and female control and STIM1Δβ mice after 10 weeks of HFD. No differences in insulin tolerance were detected between male HFD-fed control and STIM1Δβ mice or between female HFD-fed control and STIM1Δβ mice (Supplementary Fig. 2*A–C*). Given the small but significant difference in body weight and composition between female HFD-fed control and STIM1Δβ mice, metabolic cage analysis was performed. No differences in food intake, respiratory exchange rate, or total activity counts were seen between these two groups of mice (Supplementary Fig. 2*D–H*).

To test the relationship between STIM1 expression and glucose regulation in humans, we queried a publicly available data set (NCBI GEO data set *GSE50244*) that included RNA-seq results from 89 islet samples isolated from male and female organ donors with and without T2D (22). In this data set, islet STIM1 expression showed a weak but significant negative correlation with HbA_{1c} levels in female organ donors (n = 35) ($r = -0.38$; $P = 0.035$). In contrast, there was no correlation between STIM1 mRNA levels and HbA_{1c} values in male organ donors (n = 54) ($r = -0.13$; $P = 0.382$) (Fig. 1*M* and *N*).

β-Cell–Specific STIM1 Deficiency Decreases β-Cell Function and Mass in HFD-Fed Female but Not Male Mice

Our findings suggested a sexually dimorphic role for STIM1 in the regulation of glucose metabolism in both mice and humans. For determination of how loss of STIM1 impacted β-cell function in female mice, HFD-fed female control and STIM1Δβ mice were fasted for 6 h and serum insulin levels were measured 15 and 30 min after injection of glucose (2 g/kg lean mass i.p.). At 15 min after glucose injection, the increase in circulating insulin was significantly lower in female STIM1Δβ mice in comparison with control mice (Fig. 2*A*). In addition, fed insulin levels were significantly reduced in STIM1Δβ females (Fig. 2*B*).

To test whether the decrease in circulating insulin concentration was related to changes in endocrine cell composition within the pancreas, we quantitated β- and α-cell mass in pancreatic sections from female control and STIM1Δβ mice following 8 weeks of HFD. β-Cell mass was significantly reduced, while a concomitant increase in α-cell mass was observed in female STIM1Δβ mice compared with controls (Fig. 2*C–E*). Consistent with this finding, pancreatic islets isolated from HFD-fed STIM1Δβ females had significantly reduced insulin content and a trend toward increased glucagon levels ($P = 0.056$) (Fig. 2*F* and *G*). To survey granule morphology within β-cells, we performed TEM using isolated islets (Fig. 2*H*). This analysis revealed a significant increase in the fraction of immature granules (Fig. 2*I*), an increase in the ratio of immature to mature granules (Fig. 2*J*), and a significant reduction in the granule halo size in islets from STIM1Δβ female mice in comparison with their littermate controls (Fig. 2*K*).

Given the observed changes in β-cell mass and granule maturity, we next measured the expression of a panel of genes associated with β-cell function and maturity in islets isolated from female HFD-fed control and STIM1Δβ mice. Notably, we found reduced expression of markers of β-cell identity (*Slc2a2*, *Mafa*, and *Ucn3* mRNA), whereas expression of *Mafb*, a marker of α-cell identity, was significantly increased. No significant differences were found in *Nkx6.1* or *Pdx1* levels (Fig. 2*L*). Finally, analysis of glucose-stimulated Ca^{2+} responses with use of Fura-2 AM in islets revealed increased baseline activity and reduced first-phase activity in islets from HFD-fed STIM1Δβ female mice (Supplementary Fig. 3*A–D*).

No significant differences in serum or islet insulin levels, β-cell mass, α-cell mass, islet glucagon levels, or islet gene expression of β- and α-cell markers were found in HFD-fed male STIM1Δβ mice compared with their sex-matched littermate controls (Supplementary Fig. 4*A–E* and *G*).

STIM1-Deficient β-Cells Demonstrate Loss of Cellular Identity

For determination of which proteins were altered by STIM1 deletion in β-cells, unbiased tandem mass tag proteomics was performed in WT and STIM1KO INS-1 832/13 β-cell lines (15). We identified a total of 6,142 proteins in WT and STIM1KO INS-1 cells. With a cutoff of $P < 0.05$ and a Benjamini-Hochberg posttest with false discovery rate <0.05, 141 proteins were differentially expressed between WT and STIM1KO cells. Metascape analysis with enrichment values of at least 1.3 and $P < 0.05$ showed that 40 pathways were differentially regulated between WT and STIM1KO cells (23). Figure 3*A* shows the top 29 representative pathways, with terms such as "insulin signaling," "glucagon signaling," and "estrogen signaling." The most significantly changed proteins in each of these pathways are shown as a heat map in Fig. 3*B*. Notably, insulin-1 and insulin-2 expression was downregulated, while glucagon was upregulated, in STIM1KO cells (Fig. 3*B*). These results were confirmed with Western blotting, which showed reduced insulin and increased glucagon levels in STIM1KO compared with WT INS-1 cells (Fig. 3*C*).

Similar to islets isolated from STIM1Δβ mice, STIM1KO INS-1 cells demonstrated an mRNA signature of reduced β-cell maturity and identity, i.e., upregulated expression of *Gcg* and *Mafb* mRNA and reduced expression of *Mafa* mRNA (Fig. 3*D*). Next, differences in the morphology of insulin granules between WT and STIM1KO INS-1 cells were evaluated with electron microscopy. WT INS-1 cells contained insulin granules with a typical morphology characterized by dense homogeneous core and surrounding clear halo (24) (Fig. 3*E*). In contrast, STIM1KO cells had densely filled granules without the surrounding halo, an appearance more typical of glucagon-containing granules (25,26) (Fig. 3*F*).

RNA-Seq Analysis Revealed Alterations in Estrogen-Regulated Pathways in Islets From Female STIM1Δβ Mice

For further mechanistic insight into the pathways leading to β-cell dysfunction in female STIM1Δβ mice, islets

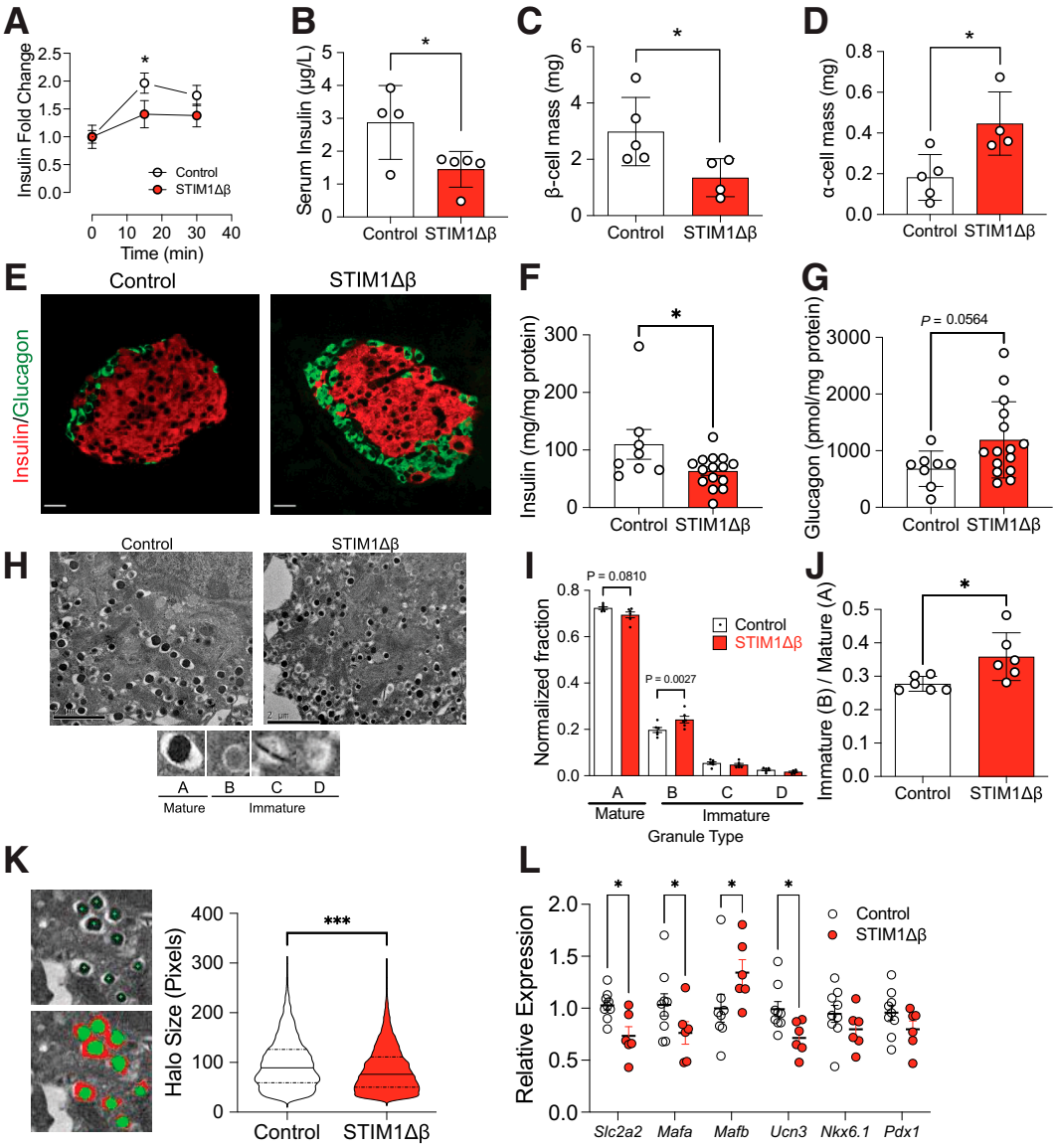

Figure 2— β-Cell–specific STIM1 deletion in female mice impairs insulin secretion under HFD conditions due to a reduction in β-cell mass and an increase in α-cell mass. *A*: After a 6-h fast, serum insulin levels were measured in control and STIM1Δβ female mice fed with HFD for 8 weeks at time 0 and 15 and 30 minutes after injection of glucose (2 g/kg i.p. glucose dosed to lean mass; $n \geq 5$ per group). *B*: Random fed serum insulin levels in HFD-fed control and STIM1Δβ female mice were determined with ELISA. *C* and *D*: Total mass of insulin-positive β-cells and glucagon-positive α-cells within pancreata was quantified in paraffin tissue sections with immunostaining for insulin and glucagon in female mice fed with HFD for 8 weeks. *E*: Representative images of islets in HFD-fed control and STIM1Δβ female mice; sections were stained with anti-insulin and anti-glucagon antibodies. *F* and *G*: Islets from animals treated with HFD for 8 weeks were isolated and lysed, and intra-islet insulin (*F*) and glucagon (*G*) protein levels were measured with ELISA. *H*: TEM analysis was performed with use of islets from female STIM1Δβ and control mice fed with HFD for 8 weeks. Granule morphology (*I* and *J*) and halo size (*K*) were assessed. *L*: mRNA levels of *Slc2a2*, *Mafa*, *Mafb*, *Unc3*, *Nkx6.1*, and *Pdx1* were analyzed with RT-qPCR in islets isolated from HFD-fed control and STIM1Δβ female mice. Results were normalized to *Actb* levels. Replicates are indicated with circles; $n \geq 4$ in each group. Results are displayed as means ± SEM. Indicated differences are statistically significant: $^*P < 0.05$.

were isolated from HFD-fed female control and STIM1Δβ mice and subjected to RNA-seq analysis. Principal components analysis showed clear separation between control and STIM1Δβ mice (Fig. 4*A*). We identified 836 differentially expressed genes based on a threshold fold-change ≥1.5 and false discovery rate <0.05. Of these, 308 genes were downregulated and 528 were upregulated (Supplementary Fig. 5*A*). Expression patterns of the top 50 differentially expressed genes (25 upregulated and 25 downregulated) are shown in Fig. 4*B*. Pathway analysis of RNA-seq data identified 55 pathways that were significantly modulated ($P < 0.05$), and 30 representative pathways are listed in Fig. 4*C*. Several pathways relevant to β-cell function and pathogenesis of T2D were identified, including "mitochondrial dysfunction," "cholesterol biosynthesis," "endocytosis," and "phagocytosis" (Fig. 4*C*). Notably, estrogen receptor signaling

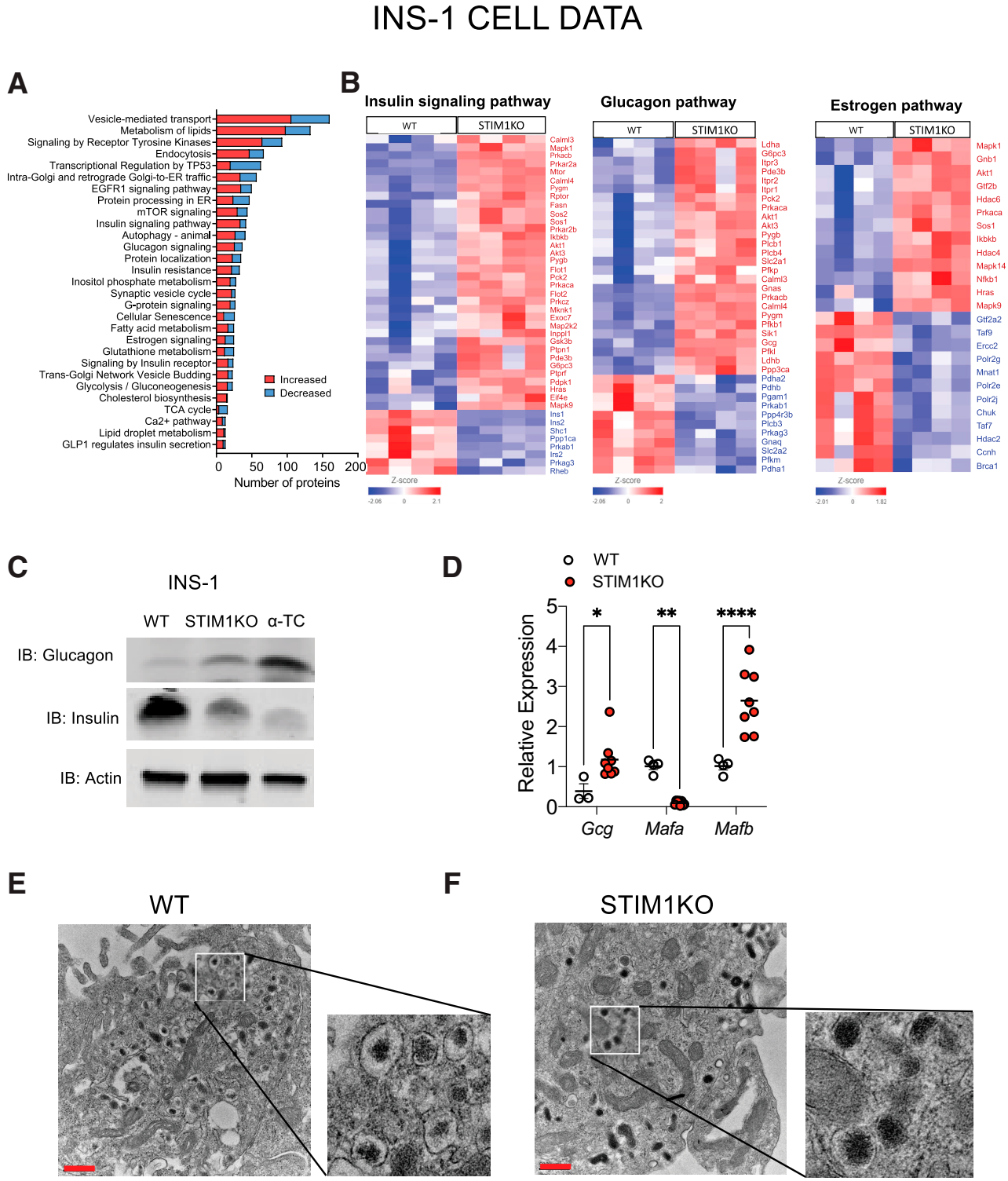

Figure 3—STIM1-deficient β-cells demonstrate loss of maturity and identity. *A* and *B*: WT and STIM1-deficient INS-1 832/13 cells (STIM1KO) were subjected to tandem mass tag MS/MS proteomics analysis. *A*: Pathway analysis was performed with Metascape; 29 representative pathways/terms are illustrated. Red and blue represent the number of increased and decreased proteins in each pathway, respectively. *B*: Abundance values of differentially expressed proteins in insulin signaling pathway, glucagon pathway, and estrogen pathway are represented in heat maps. *C*: Immunoblot (IB) analysis for glucagon, insulin, and actin in WT and STIM1KO INS-1 cells and α-TC cells. *D*: RT-qPCR for *Gcg*, *Mafa*, and *Mafb*, normalized to *Actb* levels, in WT and STIM1KO INS-1 cells. *E* and *F*: WT and STIM1KO cells were analyzed with electron microscopy. Representative images of insulin granule morphology from WT (*E*) and STIM1KO (*F*) INS-1 cells are shown (scale bar = 500 nm). Replicates are indicated with circles; $n \geq 4$ in each group. Results are displayed as mean ± SEM. Indicated differences are statistically significant; $^*P < 0.05$, $^{**}P < 0.01$, $^{****}P < 0.0001$ by one-way ANOVA (*D*). TCA cycle, tricarboxylic acid cycle.

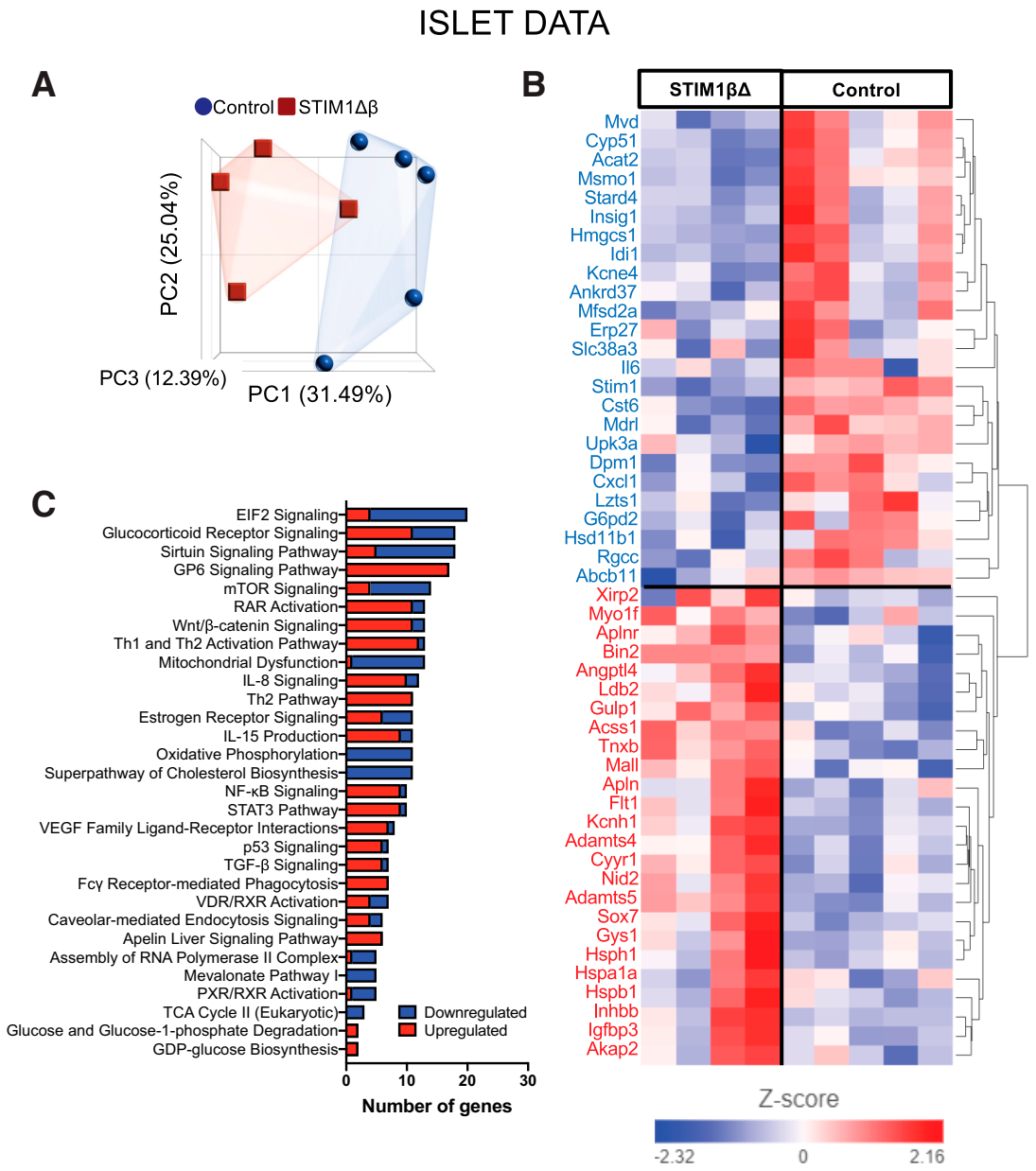

Figure 4—RNA-seq analysis revealed differential expression of genes related to pancreatic β-cell dedifferentiation in islets from female STIM1Δβ mice. *A–C*: Pancreatic islets isolated from HFD-fed control and STIM1Δβ female mice were subjected to RNA-seq analysis with use of 100 ng total RNA per sample. *A*: Principal components analysis revealed clear separation between control and STIM1Δβ islets. Log cpm values were used to generate the PCA plot. *B*: Top 50 (25 upregulated and 25 downregulated) differentially expressed genes are shown in a heat map. Blue, downregulated genes in STIM1Δβ islets; red, upregulated genes in STIM1Δβ islets. *C*: Functional enrichment analysis was performed with IPA; 20 representative pathways are illustrated. Red and blue indicate the number of up- and downregulated genes in each pathway, respectively. PC, principal component; TCA cycle, tricarboxylic acid cycle.

was also identified as a significantly modulated pathway (Fig. 4*C*). This finding was interesting, as we observed a sexually dimorphic metabolic phenotype in the STIM1Δβ mice. Therefore, we used Ingenuity Pathway Analysis (IPA) to search for potential upstream regulators of differentially expressed genes, focusing on estrogen and estrogen-related molecules and their corresponding downstream targets (Supplementary Fig. 5*B*). Twenty representative gene ontology terms obtained with the functional enrichment analysis of the identified estrogen-regulated genes are shown in Supplementary Fig. 5*C*: they include "glucagon signaling," "mitochondrial biogenesis," "G-protein–coupled receptor signaling," and "glucose metabolism." We reasoned that this novel link between STIM1 and estrogen receptor signaling could contribute to the sexually dimorphic phenotype observed in our STIM1Δβ mice.

STIM1 Deletion or Inhibition of SOCE Downregulates GPER1 Expression and Signaling in WT Mouse Islets and INS-1 Cells

Because RNA-seq showed differential regulation of estrogen-related pathways, we next analyzed the data to determine expression pattern of the three main estrogen receptors (27). The expression of estrogen receptor α and -β was unaffected (Supplementary Fig. 5*D*), while GPER1, a G-protein–coupled receptor that is an important regulator of 17-β estradiol (E2) signaling, was downregulated in STIM1Δβ islets (Fig. 5*A*). This reduction in GPER1 was confirmed at the mRNA and protein level with RT-qPCR and immunoblot analysis of islets from a separate cohort of female control and STIM1Δβ mice (Fig. 5*B–D*). For further clarification of the relationship between the regulation of ER Ca^{2+} levels and GPER1 expression, islets from WT C57Bl/6J female mice were treated with SOCE inhibitors 1-[(5-chloro-1-naphthalenyl)sulfonyl]-1,4-diazepane (ML-9), 2-aminoethoxydiphenyl borate (2-APB), or AnCoA4] for 24 h. All three inhibitors reduced the expression of GPER1 mRNA (Fig. 5*E*), indicating that SOCE is required for the maintenance of GPER1 expression in female islets. Importantly, no significant differences in GPER1 expression levels were observed in islets isolated from HFD-fed male STIM1Δβ mice and their littermate controls (Supplementary Fig. 4*F*).

To directly test the relationship between E2 signaling and STIM1, we treated WT and STIM1KO cells with 10 nmol/L E2 or G-1, an agonist of GPER1 (28). Treatment with E2 or G-1 for 15 min resulted in a 2.5-fold increase in intracellular cAMP concentration in WT INS-1 cells, indicating effective activation of this PKA-associated GPCR (Fig. 5*F*). However, the level of cAMP in STIM1KO cells remained essentially unchanged during E2 or G-1 treatment (Fig. 5*F*), confirming a defect in estrogen signaling in the absence of STIM1.

GPER1 Modulation in INS1 Cells Alters Expression of β-Cell Identity Genes and Glucagon

Finally, for testing of whether GPER1 was required for maintenance of β-cell identity, INS-1 832/13 cells were transfected with siRNA targeted to *Gper1*. Efficient knockdown of *Gper1* was confirmed with RT-qPCR (Fig. 6*A*). Markers of

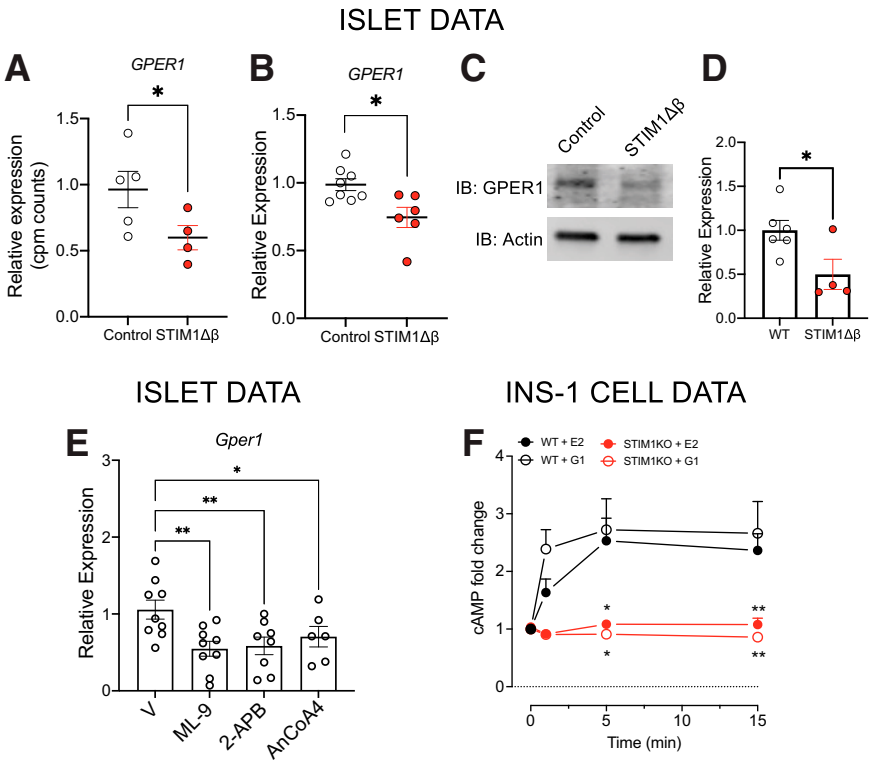

Figure 5—Inhibition of SOCE decreases expression of GPER1 in pancreatic islets and INS-1 cells. *A*: cpm counts of *Gper1* obtained from RNA-seq analysis were compared between HFD-fed control and STIMΔβ female mouse. *B*: Expression levels of *Gper1* between female control and STIM1Δβ islets were compared with RT-qPCR normalized to *Actb*. *C* and *D*: Immunoblot (IB) of GPER1 and actin from islets of HFD-fed control and STIM1Δβ female mice (*C*) and quantitation of GPER1 after normalization to actin (*D*). *E*: Islets isolated from 8-week-old C57Bl/6J female mice were treated with ML-9, 2-APB, or AnCoA4, and *Gper1* expression level was determined with RT-qPCR normalized to *Actb*. V, vehicle-treated control. *F*: Intracellular cAMP mobilization was measured with a homogeneous time-resolved fluorescence assay (HTRF). WT or STIM1KO INS-1 cells were treated with E2 (10 nmol/L) or G-1 (10 nmol/L) for 1, 5, and 15 min. The data were normalized to the baseline of the respective genotype (WT or STIM1KO). Replicates are indicated with circles; $n \geq 4$ in each group. Results are displayed as mean ± SEM. Indicated differences are statistically significant; $^*P < 0.05$, $^{**}P < 0.01$.

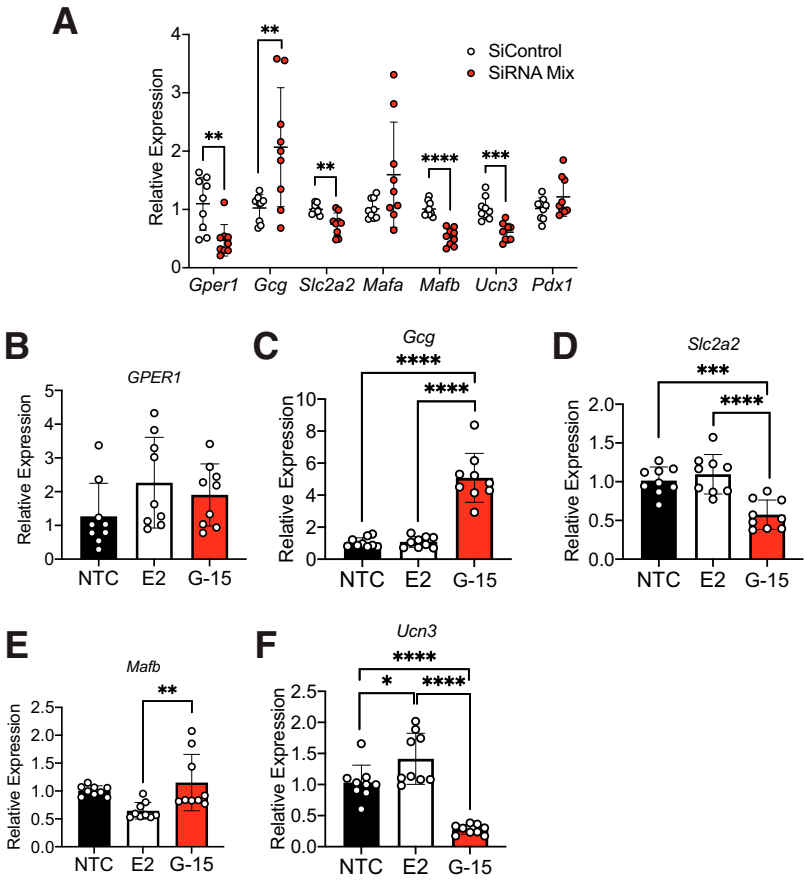

Figure 6—GPER1 knockdown and inhibition in INS-1 cells leads to a loss of β-cell identity and increased glucagon expression. *A*: INS-1 832/13 cells were transfected with small interfering (si) RNA targeted to *Gper1*. Expression of *Gper1*, *Gcg*, *Glut2*, *Mafa*, *Mafb*, *Unc3*, and *Pdx1* was measured with RT-qPCR and normalized to *Actb*. *B–F*: INS-1 832/13 cells were treated with the GPER1 agonist E2 or the GPER1 antagonist G-15. Expression of *Gper1*, *Gcg*, *Glut2*, *Mafb*, and *Unc3* was measured with RT-qPCR and normalized to *Actb*. Replicates are indicated with circles; $n \geq 9$ in each group. Results are displayed as mean ± SEM. Indicated differences are statistically significant; *$P < 0.05$, **$P < 0.01$, ***$P < 0.001$, ****$P < 0.0001$. NTC, no treatment control.

β-cell identity, including *Slc2a2*, *Mafb*, and *Ucn3*, were significantly reduced in the *Gper1* knockdown cells. Furthermore, knockdown of *Gper1* increased *Gcg* gene expression in this β-cell line (Fig. 6*A*). Consistent with the above data, treatment of INS-1 cells with E2 or with the GPER1 antagonist G-15 confirmed the changes in gene expression observed via siRNA knockdown; there was a significant decrease in β-cell identity genes *Slc2a2* and *Ucn3* and a significant increase in *Gcg* expression (Fig. 6*B–F*).

DISCUSSION

Ca^{2+} plays a vital role in normal β-cell function by regulating critical steps in insulin production, maturation, and secretion. The fidelity of many of these processes depends on the maintenance of distinct Ca^{2+} stores, organized at the cellular and organelle level. The ER serves as the dominant intracellular Ca^{2+} store, and ER Ca^{2+} depletion represents a common pathway in response to multiple metabolic stressors that contribute to diabetes pathophysiology (29–32). Under physiological conditions, reductions in ER Ca^{2+} trigger a tightly regulated rescue mechanism known as SOCE. Genetic deletion or pharmacological inhibition of SOCE or dominant-negative mutants of Orai1 or TRPC1 reduce glucose- and GPR40-mediated insulin secretion in rat islets and clonal β-cell lines (14,15,33). Interestingly, STIM1, a key component of SOCE, also regulates the activity of the sulfonylurea receptor 1 (SUR1) subunit of the K_{ATP} channel in β-cells (34), suggesting a role in insulin secretion.

We have shown that levels of STIM1 are decreased in islets from donors with T2D and that STIM1 loss is linked with β-cell ER stress (15). However, the in vivo role of STIM1 in the pathophysiology of T2D is not well established. Therefore, in this study we generated mice with a β-cell–specific STIM1 deletion (STIM1Δβ mice). At 8 weeks of age and under normal chow conditions, no significant differences in glucose tolerance were observed in either male or female STIM1Δβ mice compared with sex-matched littermate controls. However, we found that STIM1 deficiency in β-cells causes glucose intolerance and β-cell dysfunction in female, but not male, mice on HFD feeding. Further characterization of female STIM1Δβ mice revealed

that deletion of STIM1 led to impaired insulin secretion, reduced β-cell mass and identity, and increased α-cell mass. Taken together, these data suggest that STIM1 is critical for the maintenance of β-cell identity, maturity, and function in female mice.

While the sexually dimorphic pattern of glucose intolerance and β-cell dysfunction in our STIM1Δβ mice was unexpected, the preferential loss of β-cell identity in female mice has been seen in other studies. In one of the first reports to describe β-cell dedifferentiation as a component of diabetes pathophysiology, multiparous FoxO1 knockout female mice, but not male mice, had a reduction of β-cell mass and an increase in α-cell mass (35). In addition, Zhang et al. (36) demonstrated that β-cells from female Sprague-Dawley rats undergo dedifferentiation when challenged with long-term fluctuating glycemia.

Analysis of our RNA-seq data set from islets of female mice showed alterations in estrogen-related signaling pathways, raising the possibility of an underlying mechanistic connection between STIM1, β-cell differentiation/function, and sex steroids. Indeed, studies in humans and rodents have shown that an abrupt disruption of the ovarian hormonal axis via oophorectomy leads to glucose intolerance and diabetes (37,38). Some studies have suggested a similar response during natural menopause, but this remains controversial (39,40). However, 17β-estradiol (E2) signaling in rodent and human β-cells plays a protective role against diabetes stressors (27,41–43). Three estrogen receptors have been identified in the β-cell: estrogen receptor α, estrogen receptor β, and GPER1 (27). Interestingly, we found selective downregulation of GPER1 expression in STIM1Δβ female mouse islets, with preserved expression of estrogen receptor α and -β.

GPER1, also known as GPR30, belongs to a class of G-protein–coupled receptors and functions as an estrogen receptor. Several studies link GPER1 signaling to β-cell function. Islets isolated from GPER1-deficient mice demonstrate reduced glucose-stimulated insulin secretion (44), GPER1-deficient female mice are more susceptible to STZ-induced diabetes (45), and GPER1 impacts β-cell proliferation via the activity of miR-338-3p (46). The protective effect of E2 signaling in dedifferentiation of β-cells has been established, as pretreatment of islets with E2 rescued GlcN-induced β-cell dedifferentiation, and this effect was reversed by the GPER1 antagonist G-15 (47).

Our studies now show that GPER1 requires STIM1 to protect β-cells from diabetes stressors. First, we measured cAMP mobilization, a readout for GPER1 activity (48), in WT and STIM1KO INS-1 cells. As expected, cAMP levels in WT cells were significantly increased with E2 and G-1 (GPER1 agonist) treatment. However, this cAMP response was ablated in STIM1KO cells, suggesting that STIM1 is required for E2 signaling through GPER1 in β-cells. Second, we showed that siRNA-mediated knockdown of GPER1 or treatment with a GPER1 antagonist decreased the expression of markers of β-cell identity in INS-1 cells. Lastly, we showed that inhibition of SOCE decreased islet expression of GPER1. Therefore, our experiments established that STIM1 is required for GPER1-mediated protection of β-cells and maintenance of β-cell identity.

There are some limitations of our study that should be acknowledged. First, the INS-1 832/13 cell line was originally isolated from a male rat (49), and we observed a female-specific phenotype in our mouse model. However, we linked this sexual dimorphism to GPER1 signaling, and we have shown that GPER1 is expressed in INS-1 cells. Therefore, this cell line was an appropriate model for our in vitro studies. In a large data set of human islets, STIM1 expression was weakly negatively correlated with HbA_{1c} levels in female but not male organ donors. However, further studies will be needed to test the relationship between STIM1 and GPER1 signaling in human islets.

Notwithstanding these limitations, our findings show the importance of STIM1 in the maintenance of pancreatic β-cell identity in a rodent model of HFD conditions. Collectively, our data provide novel insights into potential sex differences during the development of T2D and demonstrate the importance of STIM1 and Ca^{2+} signaling in the hormonal regulation of T2D risk. On a translational note, Orai inhibitors are currently being tested for efficacy in disease states including pancreatitis, suggesting that this pathway may be amenable to therapeutic manipulation (50). Our results suggest that efforts to restore STIM1 expression or increase activation of SOCE may be considered as potential therapeutic strategies for T2D in females.

Acknowledgments. The MS experiments in this manuscript were performed in the Indiana University School of Medicine Center for Proteome Analysis. The authors thank Drs. Emma H. Doud, Amber L. Mosley, Guihong Qi, and Jaison Arivalagan (Indiana University School of Medicine) for professional support on the MS analysis. The authors also thank Dr. Emily Anderson-Baucum (freelance medical writer, Indianepolis, IN) for helpful advice and edits and Kara Orr, Lata Udari, and Jacqueline Aquino (Indiana University School of Medicine) for technical assistance.

Funding. This work was supported by National Institute of Diabetes and Digestive and Kidney Diseases (NIDDK) grants R01DK093954, R01DK127236, U01DK127786, R01DK127308, zUC4DK104166 (to C.E.-M.), and 5F30DK123996-03 (to P.S.); U.S. Department of Veterans Affairs Merit Award I01BX001733 (to C.E.-M.); and gifts from the Sigma Beta Sorority, the Ball Brothers Foundation, and the George and Frances Ball Foundation (to C.E.-M.). W.W. was supported by National Institutes of Health grant U24DK097771 as part of the NIDDK Information Network (dkNET) New Investigator Pilot Program in Bioinformatics. This work was partly supported by the Platform Project for Supporting Drug Discovery and Life Science Research from the Japan Agency for Medical Research and Development under grant no. JP23ama121001 (to T.S.). The authors acknowledge the support of the Islet and Physiology and Translation Cores of the Indiana Diabetes Research Center (P30-DK-097512).

The funders had no role in study design, data collection or analysis, decision to publish, or preparation of the manuscript.

Duality of Interest. No potential conflicts of interest relevant to this article were reported.

Author Contributions. P.S. designed and conducted the experiments, performed data analysis, and wrote the manuscript. M.R.M. conducted experiments, performed data analysis, and assisted with writing of the manuscript.

P.K. performed bioinformatics analysis on RNA-seq data, interpreted data, and edited the manuscript. W.W., M.S.R., A.T., and T.S. performed data analysis and edited the manuscript. C.-C.L. contributed to the design and execution of experiments, analyzed data, and assisted with the writing of the manuscript. T.K. contributed to funding acquisition, conception and design of the study, data analysis and interpretation, and manuscript writing and editing. C.E-M. directed the funding acquisition, designed the experiments, analyzed data, and wrote the manuscript. C.E-M. is the guarantor of this work and, as such, had full access to all the data in the study and takes responsibility for the integrity of the data and the accuracy of the data analysis.

References

1. Holman RR, Paul SK, Bethel MA, Matthews DR, Neil HA. 10-year follow-up of intensive glucose control in type 2 diabetes. N Engl J Med 2008; 359:1577–1589
2. Meier JJ, Bonadonna RC. Role of reduced β-cell mass versus impaired β-cell function in the pathogenesis of type 2 diabetes. Diabetes Care 2013; 36(Suppl. 2):S113–S119
3. Herring SJ, Oken E. Obesity and diabetes in mothers and their children: can we stop the intergenerational cycle? Curr Diab Rep 2011;11:20–27
4. Florez JC, Udler MS, Hanson RL., et al., Eds. Genetics of type 2 diabetes. In *Diabetes in America*. Bethesda, MD, National Institute of Diabetes and Digestive and Kidney Diseases, 2018
5. Kahn SE, Cooper ME, Del Prato S. Pathophysiology and treatment of type 2 diabetes: perspectives on the past, present, and future. Lancet 2014;383: 1068–1083
6. Moin ASM, Butler AE. Alterations in beta cell identity in type 1 and type 2 diabetes. Curr Diab Rep 2019;19:83
7. Bygrave FL, Benedetti A. What is the concentration of calcium ions in the endoplasmic reticulum? Cell Calcium 1996;19:547–551
8. Gilon P, Chae HY, Rutter GA, Ravier MA. Calcium signaling in pancreatic β-cells in health and in type 2 diabetes. Cell Calcium 2014;56:340–361
9. Tong X, Kono T, Anderson-Baucum EK, et al. SERCA2 deficiency impairs pancreatic β-cell function in response to diet-induced obesity. Diabetes 2016; 65:3039–3052
10. Santulli G, Nakashima R, Yuan Q, Marks AR. Intracellular calcium release channels: an update. J Physiol 2017;595:3041–3051
11. Roos J, DiGregorio PJ, Yeromin AV, et al. STIM1, an essential and conserved component of store-operated Ca2+ channel function. J Cell Biol 2005;169:435–445
12. Prakriya M, Feske S, Gwack Y, Srikanth S, Rao A, Hogan PG. Orai1 is an essential pore subunit of the CRAC channel. Nature 2006;443:230–233
13. Stathopulos PB, Zheng L, Li GY, Plevin MJ, Ikura M. Structural and mechanistic insights into STIM1-mediated initiation of store-operated calcium entry. Cell 2008;135:110–122
14. Usui R, Yabe D, Fauzi M, et al. GPR40 activation initiates store-operated Ca^{2+} entry and potentiates insulin secretion via the IP3R1/STIM1/Orai1 pathway in pancreatic β-cells. Sci Rep 2019;9:15562
15. Kono T, Tong X, Taleb S, et al. Impaired store-operated calcium entry and STIM1 loss lead to reduced insulin secretion and increased endoplasmic reticulum stress in the diabetic β-cell. Diabetes 2018;67:2293–2304
16. Sims EK, Hatanaka M, Morris DL, et al. Divergent compensatory responses to high-fat diet between C57BL6/J and C57BLKS/J inbred mouse strains. Am J Physiol Endocrinol Metab 2013;305:E1495–E1511
17. Ayala JE, Samuel VT, Morton GJ, et al.; NIH Mouse Metabolic Phenotyping Center Consortium. Standard operating procedures for describing and performing metabolic tests of glucose homeostasis in mice. Dis Model Mech 2010;3:525–534
18. Evans-Molina C, Garmey JC, Ketchum R, Brayman KL, Deng S, Mirmira RG. Glucose regulation of insulin gene transcription and pre-mRNA processing in human islets. Diabetes 2007;56:827–835
19. Fan DX, Yang XH, Li YN, Guo L. 17β-estradiol on the expression of G-protein coupled estrogen receptor (GPER/GPR30) mitophagy, and the PI3K/Akt signaling pathway in ATDC5 chondrocytes in vitro. Med Sci Monit 2018;24: 1936–1947
20. Oh-Hora M, Yamashita M, Hogan PG, et al. Dual functions for the endoplasmic reticulum calcium sensors STIM1 and STIM2 in T cell activation and tolerance. Nat Immunol 2008;9:432–443
21. Thorens B, Tarussio D, Maestro MA, Rovira M, Heikkilä E, Ferrer J. Ins1(Cre) knock-in mice for beta cell-specific gene recombination. Diabetologia 2015;58: 558–565
22. Fadista J, Vikman P, Laakso EO, et al. Global genomic and transcriptomic analysis of human pancreatic islets reveals novel genes influencing glucose metabolism. Proc Natl Acad Sci U S A 2014;111:13924–13929
23. Zhou Y, Zhou B, Pache L, et al. Metascape provides a biologist-oriented resource for the analysis of systems-level datasets. Nat Commun 2019;10: 1523
24. Fava E, Dehghany J, Ouwendijk J, et al. Novel standards in the measurement of rat insulin granules combining electron microscopy, high-content image analysis and in silico modelling. Diabetologia 2012;55:1013–1023
25. Brereton MF, Iberl M, Shimomura K, et al. Reversible changes in pancreatic islet structure and function produced by elevated blood glucose. Nat Commun 2014;5:4639
26. Powers AC, Efrat S, Mojsov S, Spector D, Habener JF, Hanahan D. Proglucagon processing similar to normal islets in pancreatic alpha-like cell line derived from transgenic mouse tumor. Diabetes 1990;39:406–414
27. Mauvais-Jarvis F, Le May C, Tiano JP, Liu S, Kilic-Berkmen G, Kim JH. The role of estrogens in pancreatic islet physiopathology. Adv Exp Med Biol 2017;1043:385–399
28. Sharma G, Hu C, Staquicini DI, et al. Preclinical efficacy of the GPER-selective agonist G-1 in mouse models of obesity and diabetes. Sci Transl Med 2020;12:eaau5956
29. Kono T, Ahn G, Moss DR, et al. PPAR-γ activation restores pancreatic islet SERCA2 levels and prevents β-cell dysfunction under conditions of hyperglycemic and cytokine stress. Mol Endocrinol 2012;26:257–271
30. Yamamoto WR, Bone RN, Sohn P, et al. Endoplasmic reticulum stress alters ryanodine receptor function in the murine pancreatic β cell. J Biol Chem 2019;294:168–181
31. Shyr ZA, Wang Z, York NW, Nichols CG, Remedi MS. The role of membrane excitability in pancreatic β-cell glucotoxicity. Sci Rep 2019;9:6952
32. Lytrivi M, Ghaddar K, Lopes M, et al. Combined transcriptome and proteome profiling of the pancreatic β-cell response to palmitate unveils key pathways of β-cell lipotoxicity. BMC Genomics 2020;21:590
33. Sabourin J, Le Gal L, Saurwein L, Haefliger JA, Raddatz E, Allagnat F. Store-operated Ca2+ entry mediated by Orai1 and TRPC1 participates to insulin secretion in rat β-cells. J Biol Chem 2015;290:30530–30539
34. Leech CA, Kopp RF, Nelson HA, Nandi J, Roe MW. Stromal interaction molecule 1 (STIM1) regulates ATP-sensitive potassium (K_{ATP}) and store-operated Ca^{2+} channels in MIN6 β-cells. J Biol Chem 2017;292:2266–2277
35. Talchai C, Xuan S, Lin HV, Sussel L, Accili D. Pancreatic β cell dedifferentiation as a mechanism of diabetic β cell failure. Cell 2012;150:1223–1234
36. Zhang J, An H, Ni K, et al. Glutathione prevents chronic oscillating glucose intake-induced β-cell dedifferentiation and failure. Cell Death Dis 2019;10:321
37. Appiah D, Winters SJ, Hornung CA. Bilateral oophorectomy and the risk of incident diabetes in postmenopausal women. Diabetes Care 2014;37: 725–733
38. Santos RS, Batista TM, Camargo RL, et al. Lacking of estradiol reduces insulin exocytosis from pancreatic β-cells and increases hepatic insulin degradation. Steroids 2016;114:16–24
39. Brand JS, Onland-Moret NC, Eijkemans MJ, et al. Diabetes and onset of natural menopause: results from the European Prospective Investigation into Cancer and Nutrition. Hum Reprod 2015;30:1491–1498

40. Ren Y, Zhang M, Liu Y, et al. Association of menopause and type 2 diabetes mellitus. Menopause 2019;26:325–330
41. Yamabe N, Kang KS, Zhu BT. Beneficial effect of 17β-estradiol on hyperglycemia and islet β-cell functions in a streptozotocin-induced diabetic rat model. Toxicol Appl Pharmacol 2010;249:76–85
42. Le May C, Chu K, Hu M, et al. Estrogens protect pancreatic beta-cells from apoptosis and prevent insulin-deficient diabetes mellitus in mice. Proc Natl Acad Sci U S A 2006;103:9232–9237
43. Alonso-Magdalena P, Ropero AB, Carrera MP, et al. Pancreatic insulin content regulation by the estrogen receptor ER alpha. PLoS One 2008;3: e2069
44. Mårtensson UE, Salehi SA, Windahl S, et al. Deletion of the G protein-coupled receptor 30 impairs glucose tolerance, reduces bone growth, increases blood pressure, and eliminates estradiol-stimulated insulin release in female mice. Endocrinology 2009;150:687–698
45. Liu S, Le May C, Wong WP, et al. Importance of extranuclear estrogen receptor-alpha and membrane G protein-coupled estrogen receptor in pancreatic islet survival. Diabetes 2009;58:2292–2302
46. Jacovetti C, Abderrahmani A, Parnaud G, et al. MicroRNAs contribute to compensatory β cell expansion during pregnancy and obesity. J Clin Invest 2012;122:3541–3551
47. Lombardi A, Ulianich L, Treglia AS, et al. Increased hexosamine biosynthetic pathway flux dedifferentiates INS-1E cells and murine islets by an extracellular signal-regulated kinase (ERK)1/2-mediated signal transmission pathway. Diabetologia 2012;55:141–153
48. Filardo EJ, Quinn JA, Frackelton AR Jr, Bland KI. Estrogen action via the G protein-coupled receptor, GPR30: stimulation of adenylyl cyclase and cAMP-mediated attenuation of the epidermal growth factor receptor-to-MAPK signaling axis. Mol Endocrinol 2002;16:70–84
49. Hohmeier HE, Mulder H, Chen G, Henkel-Rieger R, Prentki M, Newgard CB. Isolation of INS-1-derived cell lines with robust ATP-sensitive K+ channel-dependent and -independent glucose-stimulated insulin secretion. Diabetes 2000;49:424–430
50. Bruen C, Miller J, Wilburn J, et al. Auxora for the treatment of patients with acute pancreatitis and accompanying systemic inflammatory response syndrome: clinical development of a calcium release-activated calcium channel inhibitor. Pancreas 2021;50:537–543